

Bulk photogalvanic effects beyond second order

Ofir E. Alon*

Theoretische Chemie, Physikalisch-Chemisches Institut, Universität Heidelberg, Im Neuenheimer Feld 229, D-69120 Heidelberg, Germany

(Received 25 September 2002; revised manuscript received 18 December 2002; published 24 March 2003)

Examining the bulk photogalvanic effect (BPE) at nonperturbative laser fields, it is shown that illuminating a thin noncentrosymmetric crystal, quasicrystal, or nanotube the point group of which is $D_{n>2}$, $C_{(3,5,\dots)h}$, or $D_{(3,5,\dots)h}$ with a monochromatic linearly polarized field, at practically any orientation, induces a *nonvanishing* directed current component j_z along its polar axis. This is in contrast to the vanishing j_z predicted by the commonly employed photogalvanic tensor. Similarly, we discuss the appearance of an angular-dependent j_z , *already* for $C_{(n>2)v}$ and $C_{n>2}$, and circular dichroism in the BPE that are not resolved in second order. We suggest the possible observation of these currents in, e.g., thin α -quartz and $\text{LiNbO}_3:\text{Fe}$ crystals and single-walled chiral carbon nanotubes.

DOI: 10.1103/PhysRevB.67.121103

PACS number(s): 72.40.+w, 42.50.Hz, 03.65.-w, 31.15.Hz

Many nonlinear phenomena are conveniently described by expanding the electric polarization in powers of the incident radiation electric field.¹ In particular, the lowest-order nonlinear response to a monochromatic laser field is second-harmonic generation and the photogalvanic effect. In such a perturbative-based reasoning, the influence of the laser on the target is governed by physical tensors, the independent components of which are determined by the symmetry of the *bare* crystal.² The bulk photogalvanic effect (BPE) is phenomenologically described to the second order of the electric field by the expression³ ($\nu = x, y, z$)

$$j_\nu = \sum_\mu \left[\sum_\lambda \chi_{\nu\mu\lambda} \cdot \text{Re}(E_\mu E_\lambda^*) + \gamma_{\nu\mu} \cdot i(\mathbf{E} \times \mathbf{E}^*)_\mu \right], \quad (1)$$

where \mathbf{E} is the electric field vector. The linear BPE is governed by the third-rank tensor χ that transforms as the piezoelectric tensor, and is nonzero only for piezoelectric crystals.² The second-rank gyration pseudotensor γ governing the circular BPE is nonzero only in optically active crystals.² In particular, both χ and γ are identically equal to zero when the crystal possesses space inversion symmetry ($i = S_2$), i.e., the BPE occurs only in noncentrosymmetric (NCS) crystals.² Other symmetry-based properties of the BPE governed by Eq. (1) are simple to deduce from the properties of χ and γ . Such predictions, in particular angular dependencies of the BPE, have been studied and confirmed experimentally for more than 20 years now in various spatially periodic materials for intensities ranging from 10^{-8} W/cm² to about 10^8 W/cm²; see, e.g., Refs. 3–6 and references therein.

As the laser intensity is increased, higher-rank tensors of the *bare* crystal should, in principle, be taken into account, because additional powers of the electric field become non-negligible. Eventually, contributions from successive nonlinearities become comparable, and perturbation theory fails to describe the nonlinear response of the target. This brings about a relevant question as photoinduced directed currents (dcs) are considered: Do symmetry-based properties of the photogalvanic currents, in particular the (A) selection rules (SRs), (B) parameter (such as angular) dependence, and (C)

circular dichroism described by Eq. (1) persist to higher orders of the electric field? In other words, referring to property (A), can one systematically identify “forbidden” experimental geometries for which Eq. (1) rules out all or certain photocurrent components that are, nonetheless, allowed when the *full* target-laser symmetry is taken into account? To the best of our knowledge, a systematic study of *nonperturbative* symmetry-based properties of the BPE has not been performed so far. Accordingly, looking for and identifying the breakdown of the above-specified properties (A)–(C) governed by Eq. (1) have not been performed as well. Here we provide a general, simple, and *nonperturbative* method for formulating SRs for steady-state photocurrents, as well as for studying their parameter dependence and circular dichroism. Methodologically, to study the strong field *analog* of the BPE we apply our method to targets the width of which is of the order of a few tens of nanometers, and to microwave or infrared radiation. Within this widely-accepted long-wavelength–thin-target limit (see, e.g., in Refs. 7 and 8), the magnetic-component-induced effects are systematically reduced. This allows us to faithfully study, also for the irradiation intensities suggested below (10^{11} MW/cm² $\leq I < 10^{14}$ MW/cm²), the electric-component-induced dc *alone*, and thereby identifying the breakdown of the lowest-order predictions. In particular, we find that irradiating a thin NCS crystal, quasicrystal, or nanotube the point group of which is $D_{n>2}$, $C_{(3,5,\dots)h}$, or $D_{(3,5,\dots)h}$, with a monochromatic linearly polarized field, at practically any orientation, induces a *nonvanishing* dc component j_z along its polar axis, and that an angular-dependent j_z appears *already* for $C_{(n>2)v}$ and $C_{n>2}$ point groups.

Aiming at uncovering fingerprints of symmetry in the target’s response at higher laser intensities, one could proceed to evaluate symmetry properties of high-order susceptibilities, a task that becomes rather demanding for increasing orders. Here, instead, we chose to detach from the usual perturbative-based description and search for the *combined* target–laser symmetries [so-called dynamical symmetries (DSs)], which are to the time-periodic quantum system under investigation what spatial symmetries are in the stationary case.⁹ Recently, DSs were employed to study unusual SRs

for the high-order harmonic generation spectra.^{10,11} Here, identifying the DSs of the target–laser system would allow us to deduce the all-order (A)–(C) symmetry-dependent properties of the photoinduced dcs. Let us mention here that the role of spatiotemporal symmetries in ruling out nonzero average currents at asymptotic times in one-dimensional deterministically rocked periodic potentials¹² and in overdamped classical Brownian motion¹³ was recently studied.

To treat spatially-periodic and quasiperiodic targets on an equal footing, our starting point is the many-electron time-dependent Hamiltonian expressed in the momentum gauge

$$\hat{H}(\bar{\mathbf{r}}, t) = \sum_i \left\{ \frac{\left[\frac{\hbar}{i} \nabla_i - \frac{e}{c} \mathbf{A}(t) \right]^2}{2m} + V(\mathbf{r}_i) \right\} + \frac{1}{2} \sum_{i \neq k} \sum_i \frac{e^2}{|\mathbf{r}_i - \mathbf{r}_k|}, \quad (2)$$

where e and m are the electron charge and mass, respectively, $\bar{\mathbf{r}} = (\mathbf{r}_1, \mathbf{r}_2, \dots)$, $\nabla_i \equiv \partial/\partial \mathbf{r}_i$, and the summations runs over the electrons in the target. The potential $V(\mathbf{r})$ reflects the spatial symmetry of the target. Referring hereafter to the point group of the target makes the comparison to the standard second-order treatment more transparent. $\mathbf{A}(t)$ is the vector potential describing the laser field. As explained above, to analyze the strong field *analog* of the BPE we work in the long-wavelength–thin-target limit, where the spatial dependence of the vector potential in Eq. (2) can be neglected.^{7,8} Absorption of radiation by the target (a necessary condition for the linear BPE³) which lifts, of course, time-reversal symmetry, is accounted for implicitly when studying here the DSs of the target-laser system [Eq. (2)].

For time-periodic laser fields, $\mathbf{A}(t) = \mathbf{A}(t+T)$ where T is the period of the field, the solutions of the time-dependent Schrödinger equation are the so-called Floquet states¹⁴

$$\hat{H}(\bar{\mathbf{r}}, t) \psi_\varepsilon(\bar{\mathbf{r}}, t) = i\hbar \frac{\partial \psi_\varepsilon(\bar{\mathbf{r}}, t)}{\partial t}, \quad (3)$$

$$\psi_\varepsilon(\bar{\mathbf{r}}, t) = e^{-i\varepsilon t/\hbar} \phi_\varepsilon(\bar{\mathbf{r}}, t), \quad \phi_\varepsilon(\bar{\mathbf{r}}, t) = \phi_\varepsilon(\bar{\mathbf{r}}, t+T).$$

Starting from the textbook expression for the quantum-mechanical current-density,¹⁵ the many-electron photoinduced dc takes on the Floquet-based^{8,11} appearance

$$\mathbf{j} = \frac{e\hbar}{m} \text{Im} \left\{ \frac{1}{T} \int_0^T dt \int d\bar{\mathbf{r}} \phi_\varepsilon^*(\bar{\mathbf{r}}, t) \bar{\nabla} \phi_\varepsilon(\bar{\mathbf{r}}, t) \right\}, \quad (4)$$

where $\bar{\nabla} = \sum_i \nabla_i$, and $\phi_\varepsilon(\bar{\mathbf{r}}, t)$ is the Floquet state of the system. The generic case of linear combinations of Floquet states pose no special complications and the results obtained in this work remain valid for it as well. Note that the oscillating vector potential $\mathbf{A}(t)$ does not enter explicitly into photocurrent (4) within the employed dipole approximation. Of course, Eqs. (2)–(4) are gauge invariant.

To become familiar with the DS-based formalism and as a simple example, let us verify that in the nonperturbative re-

gime the *combination* of space inversion and monochromaticity also leads to $\mathbf{j} \equiv 0$ (when photon-drag effects are negligible). Under these conditions, the time-dependent Hamiltonian [Eq. (2)] possesses the second order DS

$$\hat{P}_2^{\bar{\mathbf{r}}} = \left(\bar{\mathbf{r}} \rightarrow -\bar{\mathbf{r}}, t \rightarrow t + \frac{T}{2} \right). \quad (5)$$

Thus the Floquet states $\phi_\varepsilon(\bar{\mathbf{r}}, t)$ can be classified as eigenstates of $\hat{P}_2^{\bar{\mathbf{r}}}$, namely, $\hat{P}_2^{\bar{\mathbf{r}}} \phi_\varepsilon(\bar{\mathbf{r}}, t) = \pm \phi_\varepsilon(\bar{\mathbf{r}}, t)$. Consequently, inserting $\hat{P}_2^{\bar{\mathbf{r}}}$ into expression (4) for \mathbf{j} , making use of the relation $\hat{P}_2^{\bar{\mathbf{r}}} \bar{\nabla} \hat{P}_2^{\bar{\mathbf{r}}} = -\bar{\nabla}$, leads immediately to the desired condition that $\mathbf{j} = -\mathbf{j} \equiv 0$. Following this introductory example, we now formulate the basic connection between vanishing photocurrents [Eq. (4)] and DSs: *To rule out the generation of a certain current component in a specific irradiation geometry there should exist an appropriate DS (or just spatial symmetry) that leads to the vanishing of the corresponding current component integral, Eq. (4).* Such DSs are to be associated with the field-free reflections ($\sigma = S_1$), rotations ($C_{n>1}$), and improper rotations ($S_{n>2}$), when these symmetries exist.

Let us apply the DS-based method to the monochromatic linearly polarized vector potential

$$\mathbf{A}(t; \varphi, \vartheta) = \frac{c}{\omega} \sin(\omega t) [\sin \vartheta \cos \varphi, \sin \vartheta \sin \varphi, \cos \vartheta], \quad (6)$$

where $0 \leq \varphi < 2\pi$ and $0 \leq \vartheta \leq \pi$ are the azimuthal and polar angles of the electric field with respect to the target Cartesian axes and $\omega = 2\pi/T$. The all-order SRs (L1)–(L3) for dc induced by the field (6) are listed below. In *all* but experimental geometries detailed below \mathbf{j} *does not* vanish identically. (L1) Suppose that the bare target possesses the reflection symmetry $\sigma_{\bar{z}} = (\bar{z} \rightarrow -\bar{z})$, $\bar{z} = (z_1, z_2, \dots)$, and that the electric field is linearly polarized in the x - y plane [$\vartheta = \pi/2$ in Eq. (6)]. For this setup, the time-dependent Hamiltonian [Eq. (2)] possesses the $\sigma_{\bar{z}}$ symmetry as well, and therefore the Floquet states $\phi_\varepsilon(\bar{\mathbf{r}}, t)$ can be classified as eigenstates of $\sigma_{\bar{z}}$. Substituting this observation into Eq. (4), we readily obtain that $j_z = -j_z$ and, hence, $j_z \equiv 0$. Note that on the basis of $\sigma_{\bar{z}}$ alone *no* SR can be deduced for the other two components of the photocurrent, j_x and j_y . If the electric field is linearly polarized in the z direction [$\vartheta = 0$ in Eq. (6)] then we find again $j_z = -j_z \equiv 0$, this time due to the DS:

$$\hat{P}_2^{\bar{z}} = \left(\bar{z} \rightarrow -\bar{z}, t \rightarrow t + \frac{T}{2} \right). \quad (7)$$

(L2) A similar analysis with the twofold rotation axis $C_2^{\bar{x}\bar{y}} = (\bar{x} \rightarrow -\bar{x}, \bar{y} \rightarrow -\bar{y})$ leads to $j_x \equiv 0$ and $j_y \equiv 0$ both for $\vartheta = 0$, due to $C_2^{\bar{x}\bar{y}}$ itself, and for $\vartheta = \pi/2$, due to the DS

$$\hat{P}_2^{\bar{x}\bar{y}} = \left(\bar{x} \rightarrow -\bar{x}, \bar{y} \rightarrow -\bar{y}, t \rightarrow t + \frac{T}{2} \right). \quad (8)$$

Note that on the basis of $C_2^{\bar{x}\bar{y}}$ alone *no* SR can be deduced for the j_z component, even if the electric field vector lies along or is orthogonal to the z axis. It should be emphasized that

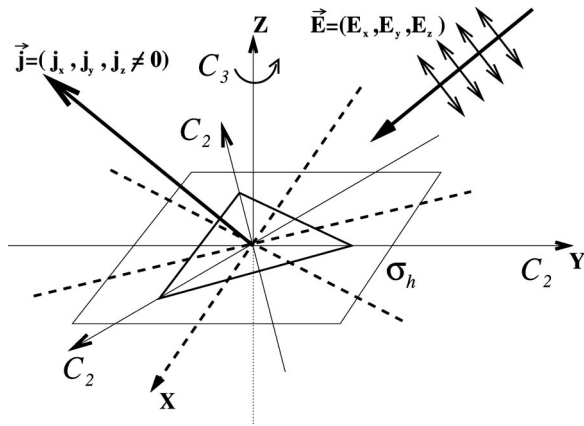


FIG. 1. Graphical illustration of generation of the “forbidden” photocurrent j_z upon illuminating a thin NCS crystal, quasicrystal, or nanotube the point group of which is $D_{n>2}$, $C_{(3,5,\dots)_h}$, or $D_{(3,5,\dots)_h}$ (here $n=3$) with a monochromatic linearly polarized field $\vec{E}=(E_x, E_y, E_z)$. For j_z to be generated for the $D_{n>2}$ point groups, the projection of \vec{E} on the x - y plane should not lie on the n “dashed” lines that are orthogonal to the n C_2 rotation axes. For j_z to be generated for the $C_{(3,5,\dots)_h}$ point groups, \vec{E} should not lie in the x - y plane ($E_z=0$) or be parallel to the z axis ($E_x=E_y=0$). For j_z to be generated for the $D_{(3,5,\dots)_h}$ point groups, the above conditions for $D_{n>2}$ and $C_{(3,5,\dots)_h}$ should be met, jointly. Evidently, at practically any orientation of the electric field \vec{E} , j_z is induced. Moreover, for a given vector \vec{E} the propagation direction is yet another degree of freedom that can be utilized to minimize the photon-drag effect when measuring j_z .

there are *no* SR’s governed by $C_{n>2}^{\vec{\varphi}}=(\vec{\varphi}\rightarrow\vec{\varphi}+2\pi/n)$, where $\vec{\varphi}=(\varphi_1, \varphi_2, \dots)$ are the azimuthal angles of the electrons, for *any* orientation of the electric field [Eq. (6)]. (L3) There is only one additional SR governed by $S_{n>2}^{\vec{\varphi}, \vec{z}}=(\vec{\varphi}\rightarrow\vec{\varphi}+2\pi/n, \vec{z}\rightarrow-\vec{z})$. If the electric field is linearly-polarized in the z direction [$\vartheta=0$ in Eq. (6)] then $j_z\equiv 0$ due to the DS $C_{n>2}^{\vec{\varphi}, \vec{z}}\hat{P}_z^{\vec{z}}=[\vec{\varphi}\rightarrow\vec{\varphi}+(2\pi/n), \vec{z}\rightarrow-\vec{z}, t\rightarrow t+(T/2)]$.

Equipped with the all-order SRs (L1)–(L3) for monochromatic linearly-polarized fields, we examined the SR’s predicted by Eq. (1) on the basis of the transformation properties of χ .² We found that they do not necessarily persist beyond second order. The central result concerns the NCS point groups $D_{n>2}$, $C_{(3,5,\dots)_h}$, $D_{(3,5,\dots)_h}$ and the field (6); also see Fig. 1. Let us start with the dihedral point groups $D_{n>2}$ that contain the C_n rotation axis (parallel to z) along with n twofold rotation axes in the x - y plane. Utilizing SR (L2), we learn that $j_z\equiv 0$ *only* if the polarization of electric field (6) is orthogonal to *any* of the n twofold rotation axes. In *all* other *continuous* set of orientations of the electric field (see Fig. 1) there is no DS and SR, and hence the j_z photocurrent component *does not* vanish. The second-order analysis, on the other hand, predicts that j_z identically vanishes, not only for the orthogonal geometries mentioned above, but also for *any* possible orientation of the field (6). Therefore, nonvanishing j_z photocurrents should appear as higher laser intensities are employed in practically *any* orientation of the electric field vector (see Fig. 1). For the point groups

$C_{(3,5,\dots)_h}$ we use SR (L1) and find similar results: $j_z\equiv 0$ *only* if the polarization of electric field (6) is in the x - y plane or is parallel to the z axis (see Fig. 1). Here again, the second-order analysis predicts that $j_z\equiv 0$ for *any* possible orientation of the field (6). Thus nonvanishing j_z photocurrents should appear as higher laser intensities are employed in practically *any* orientation of the electric field vector (see Fig. 1). Combining the results of the point groups $D_{n>2}$ and $C_{(3,5,\dots)_h}$ on the basis of SRs (L2) and (L1), respectively, gives the *continuous* geometries for which irradiation of $D_{(3,5,\dots)_h}$ leads to nonvanishing j_z along the polar axis (see Fig. 1).

The octahedral O ($n=4,3,2$) and icosahedral I ($n=5,3,2$) point groups are even more unique than the ones analyzed so far. For these point groups *all* components of the tensor χ vanish (see Refs. 2 and 16, respectively), meaning that Eq. (1) predicts $\mathbf{j}\equiv 0$ for *any* direction of electric field (6). Surprisingly, using SR (L2) we find that, unless electric field (6) is orthogonal to any of the two-fold rotation axes in O (I), *all* components of \mathbf{j} are nonzero in O (I); $\mathbf{j}\equiv 0$ only if the electric field (6) is parallel to any of the twofold rotation axes in O (I). Literally speaking, the second-order analysis almost 100% fails to describe photocurrents in O and I at higher laser intensities.

The prediction of the strong field “forbidden” photocurrents due to the combined target-laser symmetry would not be complete without arguing whether they could be detected experimentally. To argue for a positive answer, we begin by mentioning that fourth-harmonic generation was recently generated at crystalline surfaces, and moreover was used to resolve their symmetry, at peak intensities as low as $(2-5)\times 10^{11}$ W/cm².¹⁷ Detectable fifth-harmonic generation from pure silicon has been predicted at a peak intensity of about 3×10^{11} W/cm².⁷ At higher intensities of about 3.5×10^{12} and 1.3×10^{13} W/cm², according to model calculations, strong harmonic generation extending beyond the tenth and 100th harmonics has been predicted for thin (of the order of 10 nm) spatially-periodic semiconductors⁸ and for metallic single-walled carbon nanotubes,¹⁸ respectively. Moreover, Lenzner *et al.*¹⁹ recently demonstrated that sub-10-fs laser pulses open the door “to explore an entirely new—nonperturbative—regime of reversible nonlinear optics in solids,” in excess of 10^{14} W/cm². This suggests, therefore, that such “forbidden” photocurrents could be detected and resolved both in thin crystals, e.g. α -quartz (point group is D_{3h}), as well as in single-walled chiral carbon nanotubes [point groups are D_n (Ref. 20)].

Next we briefly discuss the appearance of the angular dependence in the BPE. Here we just state the final and intuitive principle: If there is *no* symmetry (say, rotation, reflection, etc.) connecting one experimental geometry to another then the corresponding photocurrent components *are not* equal. Examining the second-order predictions for $C_{(n>2)_v}$ and $C_{n>2}$, we find that the j_z is *constant* for different azimuthal angles φ [see Eq. (6)]. According to the above principle, on the other hand, this current component is φ dependent. Thus the second-order predictions cannot resolve correctly the angular-dependence of the j_z component *already* for threefold rotation symmetry. It is interesting to mention here, for comparison, that rotational analysis based

on second-harmonic generation is capable of resolving the C_{3v} symmetry at surfaces.²¹ We expect that such “forbidden” angular dependencies could be detected in thin crystals, e.g. $\text{LiNbO}_3:\text{Fe}$ (point group is C_{3v}).

Finally, let us briefly discuss the onset of circular dichroism in the BPE, i.e., when the corresponding components of photocurrents generated by circularly polarized fields of opposite helicities are not equal in their absolute values. Enquiring for the experimental geometries for which the second-order analysis fails to predict circular dichroism, we find that the point groups $D_{2(n>1)}$ exhibit circular dichroism when the polarization plane (of the circularly polarized light) contains the z axis, but does not contain any of the twofold rotation axes. Similar results are found for the point groups O and I .

In conclusion, we have found that traditional second-order predictions for symmetry-based properties of the BPE do not

persist to higher orders of the incident electric field. In particular, illuminating a thin NCS crystal, quasicrystal, or nanotube, the point group of which is $D_{n>2}$, $C_{(3,5,\dots)_h}$, or $D_{(3,5,\dots)_h}$ with a linearly polarized field, at practically any orientation, induces a *nonvanishing* dc component j_z along the polar axis. In a similar way, it has been found that j_z is *already* angular dependent for $C_{(n>2)v}$ and $C_{n>2}$. With the presently growing interest in and the capabilities of irradiating spatially periodic and quasiperiodic solid targets at non-perturbative laser intensities, our results may be of interest not only from the scientific point of view. Rather, they could find also practical applications, e.g., for the detection of microwave and infrared radiation at higher intensities.

The author wishes to thank Professor L. S. Cederbaum for stimulating discussions. O.E.A. is grateful to the European Community for financial support (Marie-Curie fellowship).

*Email address: ofir@tc.pci.uni-heidelberg.de

¹Y.R. Shen, *The Principles of Nonlinear Optics* (Wiley, New York, 1984).

²J.F. Nye, *Physical Properties of Crystals* (Oxford University Press, London, 1972).

³E.L. Ivchenko and G.E. Pikus, *Superlattices and Other Heterostructures; Symmetry and Optical Phenomena* (Springer, Berlin, 1995); B.I. Sturman and V.M. Fridkin, *The Photovoltaic and Photorefractive Effects in Noncentrosymmetric Materials* (Gordon and Breach Science, New York, 1992).

⁴V.M. Fridkin, A.A. Grekov, and A.I. Rodin, *Ferroelectrics* **43**, 99 (1982); E.L. Ivchenko and G.E. Pikus, *ibid.* **43**, 131 (1982).

⁵G. Dalba, Y. Soldo, F. Rocca, V.M. Fridkin, and Ph. Sainctavit, *Phys. Rev. Lett.* **74**, 988 (1995); S.D. Ganichev, U. Rössler, W. Prettl, E.L. Ivchenko, V.V. Bel'kov, R. Neumann, K. Brunner, and G. Abstreiter, *Phys. Rev. B* **66**, 075328 (2002).

⁶R. Atanasov, A. Haché, J.L.P. Hughes, H.M. van Driel, and J.E. Sipe, *Phys. Rev. Lett.* **76**, 1703 (1996); A. Haché, Y. Kostoulas, R. Atanasov, J.L.P. Hughes, J.E. Sipe, and H.M. van Driel, *ibid.* **78**, 306 (1997).

⁷L. Plaja and L. Roso-Franco, *Phys. Rev. B* **45**, 8334 (1992).

⁸F.H.M. Faisal and J.Z. Kamiński, *Phys. Rev. A* **56**, 748 (1997).

⁹O.E. Alon, *Phys. Rev. A* **66**, 013414 (2002).

¹⁰O.E. Alon, V. Averbukh, and N. Moiseyev, *Phys. Rev. Lett.* **80**, 3743 (1998); V. Averbukh, O.E. Alon, and N. Moiseyev, *Phys.*

Rev. A **60**, 2585 (1999); F. Ceccherini, D. Bauer, and F. Cornolti, *J. Phys. B* **34**, 5017 (2001); V. Averbukh, O.E. Alon, and N. Moiseyev, *Phys. Rev. A* **65**, 063402 (2002).

¹¹O.E. Alon, V. Averbukh, and N. Moiseyev, *Phys. Rev. Lett.* **85**, 5218 (2000).

¹²S. Flach, O. Yevtushenko, and Y. Zolotaryuk, *Phys. Rev. Lett.* **84**, 2358 (2000).

¹³P. Reimann, *Phys. Rev. Lett.* **86**, 4992 (2001).

¹⁴J.H. Shirley, *Phys. Rev.* **138**, B979 (1965); F.H.M. Faisal, *Theory of Multiphoton Processes* (Plenum, New York, 1987).

¹⁵L. I. Schiff, *Quantum Mechanics*, 3rd ed. (McGraw-Hill, Singapore, 1987).

¹⁶C. Hu, R. Wang, D.-H. Ding, and W. Yang, *Phys. Rev. B* **56**, 2463 (1997).

¹⁷Y.-S. Lee, M.H. Anderson, and M.C. Downer, *Opt. Lett.* **22**, 973 (1997); Y.-S. Lee and M.C. Downer, *ibid.* **23**, 918 (1998).

¹⁸G.Ya. Slepyan, S.A. Maksimenko, V.P. Kalosha, J. Herrmann, E.E.B. Campbe, and I.V. Hertel, *Phys. Rev. A* **60**, R777 (1999).

¹⁹M. Lenzner, J. Krüger, S. Sartania, Z. Cheng, Ch. Spielmann, G. Mourou, W. Kautek, and F. Krausz, *Phys. Rev. Lett.* **80**, 4076 (1998).

²⁰M. Damnjanović, I. Milošević, T. Vuković, and R. Sredanović, *Phys. Rev. B* **60**, 2728 (1999).

²¹B. Koopmans, F. van der Woude, and G.A. Sawatzky, *Phys. Rev. B* **46**, 12 780 (1992); S.K. Andersson, M.C. Schanne-Klein, and F. Hache, *ibid.* **59**, 3210 (1999).